Synthesis of Cobalt-Based Nanoparticles as Catalysts for Methanol Synthesis from CO_2 Hydrogenation

Anna Carrasco-García , Seyed Alireza Vali , Zahra Ben-Abbou , Javier Moral-Vico , Ahmad Abo Markeb , Antoni Sánchez *

Posted Date: 31 October 2023

doi: 10.20944/preprints202310.2044.v1

Keywords: carbon dioxide hydrogenation; methanol synthesis; nanomaterials; heterogeneous catalysis; metal-support interaction

Article

Synthesis of Cobalt-Based Nanoparticles as Catalysts for Methanol Synthesis from CO_2 Hydrogenation

Anna Carrasco-García [1], Seyed Alireza Vali [1], Zahra Ben-Abbou [1], Javier Moral-Vico [1], Ahmad Abo Markeb [1,2] and Antoni Sánchez [1,*]

[1] Departament of Chemical, Biological and Environmental Engineering, Escola d'Enginyeria, Universitat Autònoma de Barcelona, 08193 Cerdanyola del Vallès, Barcelona, Spain; anna.carrasco@uab.cat (A.C.G.); Seyedalireza.vali@uab.cat (S.A.V.) zahra.benabbou@autonoma.cat (Z.B.A); antoniojavier.moral@uab.cat (J.M.-V.); a_markeb@aun.edu.eg (A.A.M.); antoni.sanchez@uab.cat (A.S.)

[2] Departament of Chemistry, Faculty of Science, Assiut University, Assiut 71516, Egypt

* Correspondence: Antoni.sanchez.@uab.cat

Abstract: The increading emission of carbon dioxide to the atmosphere has urged the scientific community to investigate alternatives to alleviate such emissions being the principal contributor to the greenhouse gas effect. One major alternative is carbon capture and utilisation (CCU) towards the production of value-added chemicals using diverse technologies. This work aims at the study of the catalytic potential of different cobalt-derived nanoparticels for methanol syntheis from carbon dioxide hydrogenation. Thanks to its abundance and cost-efficacy, cobalt can serve as an economical catalyst compared to noble-metal-based catalysts. In this work, we present a systematic comparison among different cobalt and cobalt oxide nanocomposites in terms of their efficiency as catalysts for carbon dioxide hydrogenation to methanol as well as how different supports can enhance their catalytic capacity. The oxygen vacancies in the cerium oxide act as carbon dioxide adsorption and activation sites, which facilitates a higher methanol production yield.

Keywords: carbon dioxide hydrogenation; methanol synthesis; nanomaterials; heterogeneous catalysis; metal-support interaction

1. Introduction

Nowadays, one of the main worldwide concerns is the slow but unstoppable rise in global average temperature, a direct cause of climate change that seems almost unavoidable. The high quantities of greenhouse gases emitted to the atmosphere, of which carbon dioxide emissions are the most important, predict an increase in the Earth's temperature by 2040 of approximately 1.5 ºC compared to the data recorded at the end of the 19th century [1]. Such predictions have alerted the scientific community to develop protocols to lower carbon dioxide emissions, which can be classified according to whether they are carbon capture and storage (CCS) or carbon capture and utilization (CCU) methods. On one hand, CCS methods consist of capturing and storing the gas, and it is so efficient that it could account for almost 20% of the carbon dioxide reduction. Nevertheless, it can result quite costly because industrial-scale installations have to be built. Unfortunately, fossil fuels are still needed as an energy source for this treatment, so carbon dioxide reduction will never be fully completed [2].

On the other hand, CCU results are remarkably interesting, since it does not only deals with the storage of carbon dioxide, but it takes advantage of this gas as a valuable carbon resource for chemical conversion into other products. This is a more viable strategy as it could not only keep the atmospheric concentration at acceptable levels, but also provides high added-value chemical/fuel products, such as methane and methanol [3,4]. Among all the technologies, carbon dioxide hydrogenation has been considered a promising alternative for obtaining some products from carbon dioxide. An attractive possibility is the production of methanol, a chemical compound that has a wide range of applications. For instance, it can be used as a solvent to obtain several chemicals

Preprints (www.preprints.org) | NOT PEER-REVIEWED | Posted: 31 October 2023 doi:10.20944/preprints202310.2044.v1

(formaldehyde, acetic acid, etc.), as well as in the conversion process to olefins, which can be used to produce hydrocarbon fuels and their derivatives, which are currently obtained from petroleum [5,6].

The hydrogenation of carbon dioxide to methanol consists of two main competing reactions. The first is the synthesis of methanol from carbon dioxide and hydrogen:

$$CO_2 + 3H_2 \rightarrow CH_3OH + H_2O \quad \textbf{Equation 1} \qquad \Delta H^0{}_{298\,K} = -49.5\ kJ/mol$$

The second reaction is the reverse water-gas shift reaction (RWGS), which produces carbon monoxide:

$$CO_2 + H_2 \rightarrow CO + H_2O \quad \textbf{Equation 2} \qquad \Delta H^0{}_{298\,K} = 41.2\ kJ/mol$$

Furthermore, catalytic hydrogenation of carbon dioxide into methanol can also occur indirectly from carbon monoxide formed through the RWGS reaction [7]:

$$CO + 2H_2 \rightarrow CH_3OH \quad \textbf{Equation 3} \qquad \Delta H^0{}_{298\,K} = -90.6\ kJ/mol$$

The synthesis of methanol is thermodynamically favoured at low temperatures and high pressures [8,9].

In recent years, bimetallic catalysts have been extensively investigated due to their chemical, electronic and structural properties, as well as the synergistic effects between metals leading to the catalytic system. Unlike monometallic systems, the bimetallic catalytic system has advantages in terms of selectivity, activity and stability [10]. The catalysts mainly chosen for carbon dioxide hydrogenation to methanol studies are Cu-Zn based systems, although other bimetallic catalysts such as Pd-Zn, Pd-Ga, Cu-Ni and Ni-Ga have been also investigated [7]. In addition to these mentioned catalysts, methanol has also been obtained using cobalt-based catalysts. Stangeland et al. [11] demonstrated that Co_3O_4/MnOx was efficient in the production of methanol at mild pressures, but a variety of by-products are also obtained. These authors achieved a 10-fold increase in methanol yield with Co_3O_4/MnOx catalysts compared to Cu/Zn based catalysts under similar conditions [11]. Wang et al. [12] investigated silica-supported cobalt catalysts with the aim of accelerating the selectivity of the hydrogenation of carbon dioxide to methanol, and they showed that the inclusion of silica in the cobalt catalysts improved both carbon dioxide conversion and selectivity towards methanol [12].

One of the key aspects of cobalt-based catalysts is their ability to catalyse various carbon dioxide conversion reactions, including methanation [13,14], synthesis of higher alcohols [15,16] or methanol synthesis [11,12,17,18]. In these investigations, it was shown that the selectivity of these catalysts can be influenced by the use of different supports. In the present study, different supports including zeolite, manganese oxide and cerium oxide have been investigated to increase the catalytic activity of cobalt-based catalysts. It is hypothesiezed that different metal-support interactions between cobalf nanoparticles and the support will enhance the catalytic sites, leading to higher methnaol yield and selectivity. Zeolite is a microporous aluminosilicate with a three-dimensional structure based on SiO_4 and AlO_4 and it is known for its catalytic and adsorption properties [19]. Cerium oxide is a non-toxic oxide, which is of great importance in catalysis, due to its ability to store and supply oxygen [20,21]. It provides a large number of oxygen vacancies on the surface which can fucntion as sites for adsorption and activation of carbon dioxide. Manganese oxide is a mesoporous support like zeolite and cerium oxide its efffect as support for nanocatalysts used for carbon dioxide hydrogenation to methanol has not been reported [11].

On the other hand, capping agents are of utmost importance as stabilisers since they counteract the attraction between nanoparticles, thus inhibiting their overgrowth and aggregation. These agents are amphipathic molecules that are characterized by having a polar head group and a non-polar tail, and due to this amphipathic property, they improve the compatibility with other phases. Different types of protection agents have been implemented in the synthesis of nanomaterials (surfactants, polymers, polysaccharides, etc.), aiming to obtain nanoparticles of smaller sizes, which will lead to the highest surface area of the nanoparticles [19,22]. In this study, the agglomeration of the synthesized nanoparticles was controlled by steric stabilisation using polyvinylpyrrolidone (PVP).

 doi:10.20944/preprints202310.2044.v1

The present work is focused on studying the catalytic activity of supported and unsupported cobalt-based nanoparticels. The aim is to evaluate this type of nanomaterials in order to obtain high methanol production yields and high selectivity under mild pressure and temperature conditions.

2. Materials and Methods

2.1. Materials

Sodium borohydride ($NaBH_4$) (99.0%), cobalt (II) chloride hexahydrate ($CoCl_2{\cdot}6H_2O$) (99.0%), polyvinylpyrrolidone (PVP), sodium carbonate (Na_2CO_3) (99.5%), zeolite, cerium (III) nitrate hexahydrate ($Ce(NO_3)_3{\cdot}6H_2O$ (99.0%), sodium hydroxide (NaOH) (98.0%), manganese (II) sulphate monohydrate ($MnSO_4{\cdot}H_2O$) (99.0%), and potassium permanganate ($KMnO_4$) (99.5%) were all purchased from Sigma-Aldrich (Barcelona, Spain). A mixed-gas bottle of carbon dioxide and hydrogen with a molar ratio of 1:3, respectively, was provided by Carburos Metálicos S.A. (Barcelona, Spain).

2.2. Synthesis of nanocomposites

2.2.1. Co nanoparticles synthesis

Co nanoparticles were synthesized using the chemical reduction method. A total of 1.10 g of cobalt (II) chloride hexahydrate was dissolved in a beaker with 100 mL of deionised water with magnetic stirring and nitrogen bubbling to avoid the oxidation of cobalt. After 15 min of stirring, the reducing agent, sodium borohydride, was added. A total of 0.96 g of sodium borohydride was dissolved in 100 mL of deionised water and then added dropwise with a Pasteur pipette. Once the reducing agent was added, the solution was left to stir for 20 min to ensure that all of the cobalt had been reduced [23]. Once the reaction was complete, cobalt nanoparticles were separated from the water using a magnet. The product was washed three times with deionised water to remove any impurities and dried in an oven at 105 ºC overnight. The synthesis of Co nanoparticles with PVP was performed with the same method, but 1.10 g of PVP was added to the cobalt (II) chloride hexahydrate solution.

2.2.2. Co_3O_4 nanoparticles synthesis

Co_3O_4 nanoparticles were synthesized using the co-precipitation method. Briefly, in 100 mL of deionised water, 0.61 g of cobalt (II) chloride hexahydrate was dissolved using magnetic stirring for 20 min and in another 100 mL of deionised water was dissolved the precipitation agent, 0.52 g of sodium carbonate at a concentration of 1 M. The synthesis was performed in a 500 mL Scharlau Minireactor HME-R/500 with mechanical stirring and heating. The 100 mL cobalt (II) chloride hexahydrate solution in deionised water was added to the reactor. Then, the NaOH solution was added at a flow rate of 5 mL/min using a peristaltic pump (Watson Marlow SCI 400), and the reaction was carried out at 60 ºC for 5 h with constant stirring at 120 rpm. The product was centrifuged (Beckman Avanti J-20 Centrifuge) three times for 15 min at 5000 rpm to remove any impurities and dried in an oven at 105º C overnight [23]. The synthesis of Co_3O_4 with PVP was performed with the same method, but 0.62 g of PVP was added to the cobalt (II) chloride hexahydrate solution.

2.2.3. MnO_2 nanoparticles synthesis

MnO_2 nanoparticles were synthesized using the co-precipitation method. In 100 mL of deionised water, 3.12 g of manganese (II) sulphate monohydrate were dissolved and in another 100 mL of deionised water 2.18 g of potassium permanganate were dissolved. The potassium permanganate dissolution was added to the above dissolution dropwise, and the mixture was vigorously stirred in a reactor Scharlau Minireactor HME-R/500 (Barcelona, Spain) at 80 ºC for 5 hours. Then, a sodium hydroxide solution was added dropwise to adjust the pH to 11. Once the reaction was completed, the

 doi:10.20944/preprints202310.2044.v1

nanoparticles were centrifuged and washed three times with deionised water. Finally, the nanoparticles obtained were dried at 105 ºC for 12 hours [24].

2.2.4. Co_3O_4/Zeolite nanocomposite synthesis

To immobilize the Co_3O_4 nanoparticles onto zeolite the same Co_3O_4 synthesis described above was followed. In 200 mL of ultrapure water, 1 g of zeolite was dispersed in an ultrasound bath for 15 minutes. Once zeolite was dispersed, it was transferred to the reactor, and the same Co_3O_4 synthesis procedure was performed.

2.2.5. CeO_2 nanoparticle synthesis

CeO_2 nanoparticles were synthesized using the co-precipitation method from an aqueous solution of cerium (III) nitrate hexahydrate. In 100 mL of deionised water, 5.12 g of cerium (III) nitrate hexahydrate were dissolved, and in another 100 mL of deionised water 1.88 g of the precipitant agent, sodium hydroxide, were dissolved. The synthesis was carried out in a reactor (Scharlau Minireactor HME-R/500) with mechanical agitation. The precursor solution and 100 mL of deionised water was added to the reactor, and then, by a peristaltic pump, the sodium hydroxide solution was added with a 7mL/min flow. Once the entire precipitating agent was added, the dissolution was left agitating for 15 minutes. Eventually, the precipitates obtained were leaked, washed with deionised water three times, and then dried at 105 ºC overnight [25].

2.2.6. Co_3O_4 /CeO_2 nanocomposite synthesis

To immobilize the Co_3O_4 nanoparticles onto CeO_2, the same Co_3O_4 synthesis procedure was followed. In 200 mL of deionised water, the nanoparticles of CeO_2 were scattered in an ultrasound bath for 15 minutes. Once dispersed, the same Co_3O_4 synthesis procedure was carried out, but first the solution of the CeO_2 nanoparticles was transferred to the reactor.

2.2.7. Co_3O_4 /MnO_2 nanocomposite synthesis

Co_3O_4 nanocomposites were synthesized using the co-precipitation method. The same Co_3O_4 synthesis procedure followed, but first the previously synthesized MnO_2 nanoparticles were dispersed in 200 mL of deionised water in an ultrasound bath for 15 minutes. Subsequently, the same Co_3O_4 synthesis was followed after the dissolution of MnO_2 was added to the reactor.

2.3. Characterization of catalysts

X-ray diffraction (XRD) was used to perform a structural analysis of the nanoparticles and their crystallographic structure. The X-ray diffraction patterns were recorded on a diffractometer (PANalytical X'Pert) using Cu-Kα radiation. The measurements were carried out at room temperature in a range of 10.0º - 80.0º on 2θ with a step size of 0.026º. All XRD results were analysed with the simulation of the nanoparticles obtained using the X'Pert High Score (PANalytical) software. A scanning electron microscopy (SEM) (FEI Quanta 650F ESEM) equipped with an energy-dispersive spectroscopy (EDS) source was used to determine the morphology, size distribution and composition of the nanoparticles. Samples were prepared on copper and graphite grids (TED PELLA, Inc., Redding, CA, USA).

2.4. Catalytic activity test

The catalytic experiments were carried out in a stainless-steel-packed bed reactor with an internal diameter of 5.25 mm, a height of 8.90 cm, and, thus, a volume of 1.92 cm^3. All samples were calcinated at 500 °C for 4 h and and those containing elemental copper were reduced by a hydrogen flow of 40 mL/min at 350 °C for 2h. A certain amount of catalyst was added and a small amount of glass wool was used at each end of the reactor to avoid possible leakage of the catalysts. In order to investigate the impact of pressure, the work was carried out under two moderate pressure values: 10

Preprints (www.preprints.org) | NOT PEER-REVIEWED | Posted: 31 October 2023 doi:10.20944/preprints202310.2044.v1

and 15 bar. The flow rate of the stoichiometric H_2/CO_2 mixture was 10 mL/min, and the effect of temperature on the catalytic activity of the catalyts was tested by changing the temperature ranging from 180 to 280 °C. The gas samples were collected using sampling bags (SKC FlexFoil PLUS Sample Bag), and the obtained methanol was analysed in a gas chromatograph (Shimadzu GC-2010) with a flame ionisation detector (FID) using helium as carrier gas. The software used was Chromeleon, the inlet temperature was 260 °C, and the flow was 50 mL/min; the detector temperature was 280 °C. An Agilent 7890B GC System chromatograph served to detect carbon monoxide and dioxide by using a thermal conductivity detector (TCD) with helium as the carrier gas. The software used was OpenLab, the inlet temperature was 120 °C, the inlet flow was 20 mL/min and the detector temperature was 150 °C. To study the catalytic activity, methanol space–time yield (STY) indicating the mass of methanol obtained per mass of catalyst per hour as well as methanol selectivity being the percentage of carbon dioxide that was converted to methanol rather than other products (in this case carbon monoxide) were caclulated accrding to the following equations.

$$CH_3OH\ STY\ \left(\frac{g}{kg_{cat}\times h}\right)=\left(\frac{Mass\ of\ methanol\ (g)\ formed}{W_{cat}(kg)\times Hour}\right) \quad (1)$$

$$CH_3OH\ Selectivity\ (\%)=\left(\frac{moles\ of\ methanol\ formed}{n[CO_2]_{in}-n[CO_2]_{out}}\right)\times 100 \quad (2)$$

3. Results and Discussion

3.1. Structural and morphological characterization of nanomaterials

The XRD patterns obtained for cobalt and cobalt oxide with and without capping aganet (PVP) and their corresponding simulations using PANALYTICAL X'Pert High Score software are presented in Figure 1. As it is shown, the peaks at diffraction angles of 2θ of 19.05º, 31.27º, 36.90º, 38.56º, 44.82º, 55.70º, 59.40º, 65.30º, 74.14º and 77.14º correspond to the (111), (220), (311), (222), (400), (422), (511), (440), (620) and (533) planes of Co_3O_4 [11,23,26]. Furthermore, the peaks at 2θ of 44.23º (111), 51.52º (200) and 75.85º (220) corresponed to Co nanoparticles [23]. Regarding the Co_3O_4 and Co with and without PVP, it was observed that PVP did not interfere with the crystallinity of cobalt and cobalt oxide nanoparticles. As can be seen, there is no presence of cobalt oxide in the cobalt XRD patterns, indicating that the synthesis of cobalt nanoparticels was satisfactory and all the nanoparticles were completely reduced.

Preprints (www.preprints.org) | NOT PEER-REVIEWED | Posted: 31 October 2023 doi:10.20944/preprints202310.2044.v1

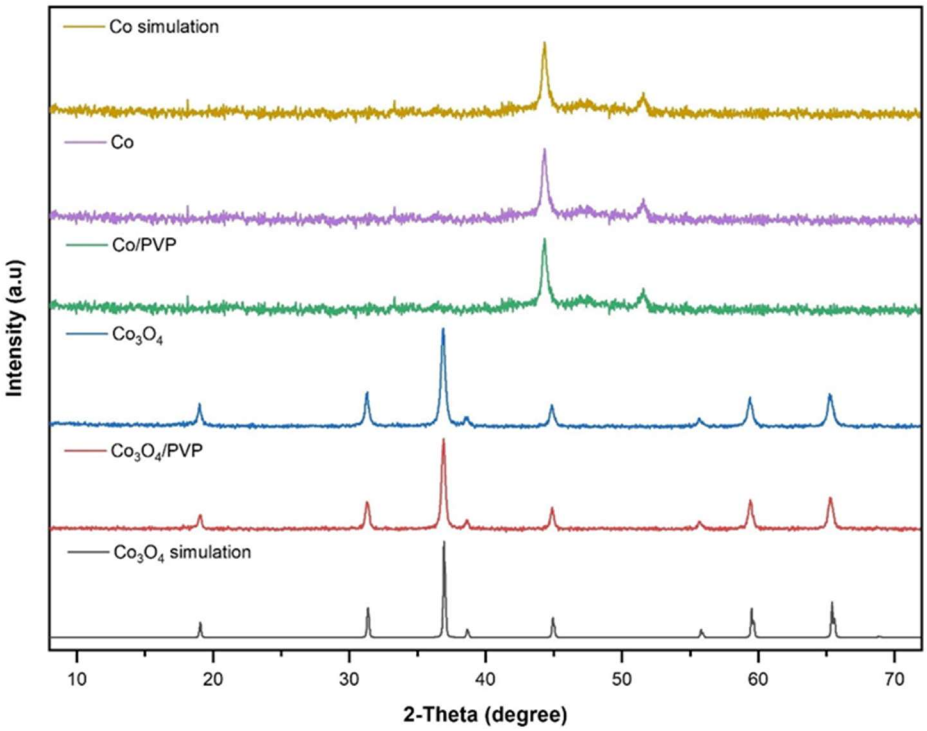

Figure 1. XRD patterns of all catalysts: Co simulation; Co nanoparticles; Co/PVP nanoparticles; Co_3O_4 nanoparticles; Co_3O_4/PVP nanoparticles; Co_3O_4 simulation.

The X-ray diffraction patterns of all the supports are shown in Figure 2. Regarding the first support, CeO_2, it is observed that the peaks obtained in the sample synthesized and the simulation are identical. The same phenomenon occurs with zeolite. However, not all the peaks observed in the MnO_2 simulation correspond to the peaks observed in the synthesized sample, which indicates that this sample is not completely crystalline.

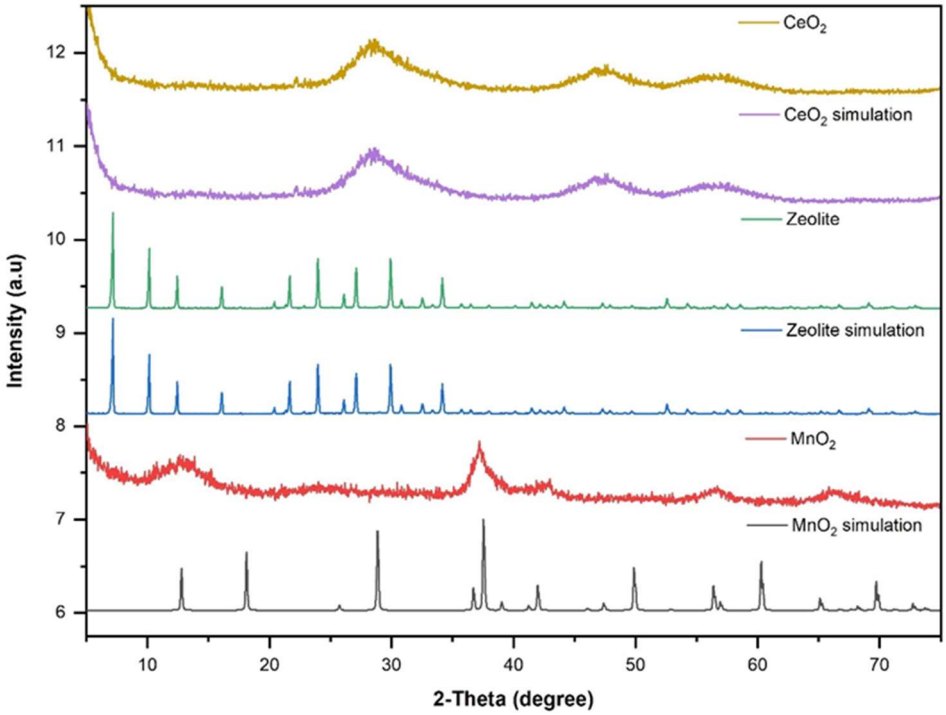

Figure 2. XRD patterns of all catalysts: CeO_2; CeO_2 simulation; Zeolite; Zeolite simulation; MnO_2; MnO_2 simulation.

Preprints (www.preprints.org) | NOT PEER-REVIEWED | Posted: 31 October 2023 doi:10.20944/preprints202310.2044.v1

The X-ray diffraction patterns of the bimetallic nanoparticles and their supports are shown in Figure 3. Regarding the highest peaks of Co_3O_4/zeolite, it is observed that the first peaks are associated to zeolite since the X'Pert High Score software determined that they correspond to the two typical elements of zeolite (aluminum and silicon). Small peaks corresponding to Co_3O_4 were also observed at the following angles: 19.05º, 31.27º, 36.90º, 38.56º, 44.82º, 55.70º , 59.40º and 65.30º. Regarding the XRD patterns of Co_3O_4 /CeO_2, it is observed that the peaks situated at the angles 28.50º, 33.10º, 47.50º, 56.30º, 69.40º, 76.70º and 79.10º belong to CeO_2. They are associated with planes (111), (200), (220), (311), (400), (331) and (420), respectively (Figure 3) [27]. Moreover, other characteristic peaks of Co_3O_4 are seen at angles 19.05º, 31.27º, 36.90º, 38.56º, 44.82º and 65.30º (Figure 3) [28]. Finally, in the Co_3O_4/MnO_2 patterns, the peaks of both materials can also be visualised (Figure 3). The angles 24.50º, 41.60º, 50.30º, 54.70º, 63.70º, 72.30º and 79.19º correspond to Co/MnO_2, and are related to the (110), (120), (220), (231), (130), (343) and (330) planes (Figure 3) [29]. Nevertheless, the other profiles observed correspond to the cobalt oxides present in the sample, since they coincide with the Co_3O_4 angles described above. This means that there is a coexistence of elemental cobalt and its oxidized species in the sample.

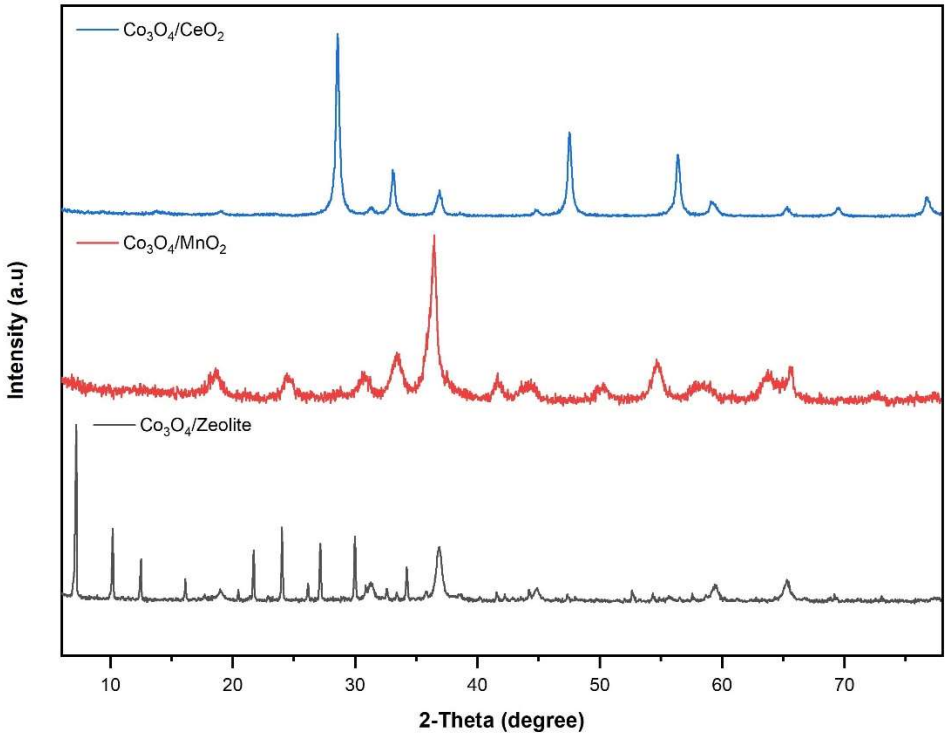

Figure 3. XRD patterns of all catalysts: Co_3O_4/CeO_2; Co_3O_4/MnO_2; Co_3O_4/zeolite.

The characterization and morphology study of the materials was performed using a scanning electron microscope (SEM). Figure 4C shows the SEM images of the Co_3O_4 nanoparticles, which presented an irregular shape with a high degree of agglomeration, with average sizes of 36-64 nm, as previously reported [23]. Nevertheless, when the PVP was added, the nanoparticles were smaller (19 - 25 nm) with a more spherical geometry (Figure 4D). It is reported in literature that by adding a capping agent, the nanoparticles are smaller and this effect leads to an increase in the surface area of the catalyst, which means that the active sites are more exposed. Therefore, the catalytic activity of the catalyst increases [19,22]. The morphology of cobalt nanoparticles with and without PVP is shown in Figure 4A and Figure 4B, respectively. The same effect is observed when PVP was added to the synthesized material: the morphology obtained is well defined and the particles are smaller.

Preprints (www.preprints.org) | NOT PEER-REVIEWED | Posted: 31 October 2023 doi:10.20944/preprints202310.2044.v1

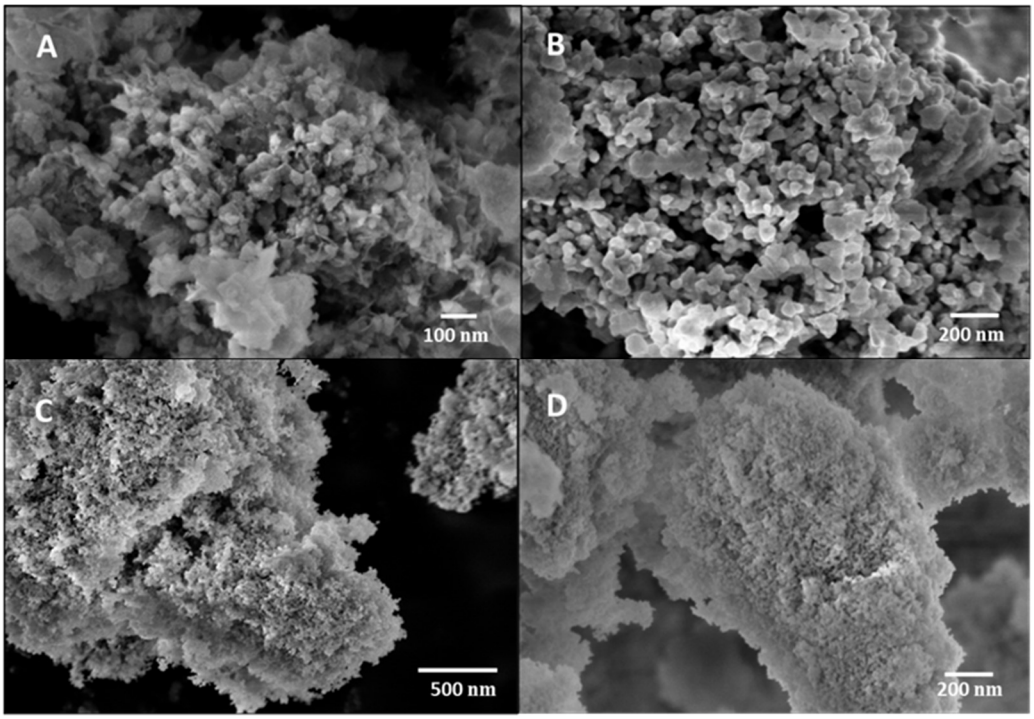

Figure 4. SEM images of the catalysts: (**A**) Co nanoparticles; (**B**) Co/PVP nanoparticles; (**C**) Co_3O_4 nanoparticles; (**D**) Co_3O_4/PVP nanoparticles.

SEM images of nanoparticles embedded in a support are presented in Figure 5. Co_3O_4 nanoparticles immobilised on zeolite show a granular morphology with an average diameter of 24-30 nm (Figure 5A). It is shown that the use of support helps to obtain nanoparticles with better distribution and a higher surface area. In Figure 5C, Co_3O_4 nanoparticles supported on CeO_2 can be observed, demonstrating that the nanoparticles have a very small size and better distribution compared to Co_3O_4 nanoparticles without support (Figure 4C) [28]. Co_3O_4 nanoparticles embedded in MnO_2 show an aggregated morphology, as previously reported in literature (Figure 5B) [24].

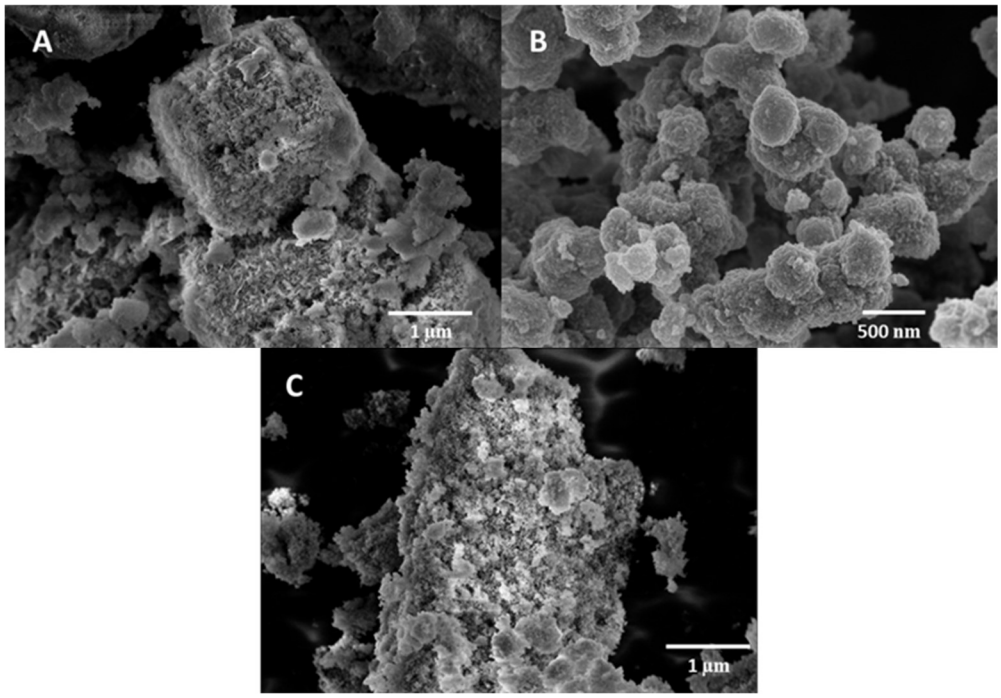

Figure 5. SEM images of the catalysts: (**A**) Co_3O_4/Zeolite; (**B**) Co_3O_4/MnO_2; (**C**) Co_3O_4/CeO_2.

Preprints (www.preprints.org) | NOT PEER-REVIEWED | Posted: 31 October 2023 doi:10.20944/preprints202310.2044.v1

The composition of the chemical elements present in the catalysts was determined by energy dispersive spectrometry (EDX). This analysis was performed on the nanoparticles immobilised on the three tested different supports. As observed with XRD, the EDX spectrum of Co_3O_4/Zeolite confirms the presence of expected chemical elements (Co, Al, Si) (Table 3) [30]. Nevertheless, a very small presence of sodium from the reducing agent used during the synthesis was also detected, indicating that the material could have been washed more times. Co and Ce were detected in the Co_3O_4/CeO_2 sample, as expected (Table 2). In the Co_3O_4/MnO_2 sample (Table 1), the presence of Co and Mn elements was detected, as well as a very small amount of sodium and potassium.

Table 1. Element quantification with EDX of Co_3O_4/MnO_2 material.

Element	Weight (%)	Atomic (%)
C	28.60	43.21
O	38.52	43.68
Mn	14.38	4.75
Co	14.15	4.36
Na	0.54	0.42

Table 2. Element quantification with EDX of Co_3O_4/CeO_2 material.

Element	Weight (%)	Atomic (%)
C	5.44	16.78
O	24.06	55.74
Co	21.43	13.48
Ce	48.46	12.82

Table 3. Element quantification with EDX of Co_3O_4/Zeolite material.

Element	Weight (%)	Atomic (%)
C	46.01	58.85
O	35.51	34.10
Si	2.12	1.16
Al	2.25	1.28
Co	11.83	3.08
Na	2.29	1.53

3.2. Catalytic activity of the catalysts

To study the catalytic activity of the samples, methanol STY and selectivity were obtained. Figure 6 presents methanol STY for cobalt and its oxide as a function of operating temperature at pressures of 10 and 15 bar, respectively. The effect of reaction temperature was also investigated and as can be seen for most of the catalysts methnaol STY increases gradually as the temperature rises. However, for Co_3O_4 catalyst, a decrease in STY was observed at 280 ºC compared to 260 ºC, which is not in accord to the behaviour of other catalysts. This can attributed to the formation of more carbon monoxide at high temperatures due to the endothermic nature of reverse water gas shoft reaction as the competeing reaction for methnaol syntheis as presented before. The influence of pressure was also investigated, and the results showed that a better catalytic activity is obtained at 15 bar, as the use of high pressures is advantageous due to the exothermic nature of the reaction [8,11].

Furthemore. the catalytic activity of cobalt and cobalt oxide was compared in terms of STY and selectivity to understand which cobalt species presents the active sites more favorable for methnaol synthesis. As can be observed, cobalt nanoparticles give methnaol STY of 3.2 $g.kg_{catalyst}^{-1}h^{-1}$, while only 0.25 $g.kg_{catalyst}^{-1}h^{-1}$ was obtained for cobalt oxide nanoparticles. Hence, metalic cobalt posseses active sites catalyzing the methnaol syntheis from carbon dioxide hydrogenation reaction more efficiently. Using elemental Co, a higher STY was obtained if compared to Co_3O_4 catalyst, since the selectivity of the reaction is much more favoured for methanol formation than for carbon monoxide production

Preprints (www.preprints.org) | NOT PEER-REVIEWED | Posted: 31 October 2023 doi:10.20944/preprints202310.2044.v1

when this material is used instead of Co_3O_4, because the latter material is highly selective towards methane and carbon monoxide formation [31,32]. In many studies, this effect has been attributed to a lower carbon dioxide adsorption on the cobalt surface compared to Co_3O_4, which favours the formation of other products such as methane when using the oxide [33]. However, the catalyst selected for the study was cobalt oxide due to its high stability compared to elemental cobalt [35].

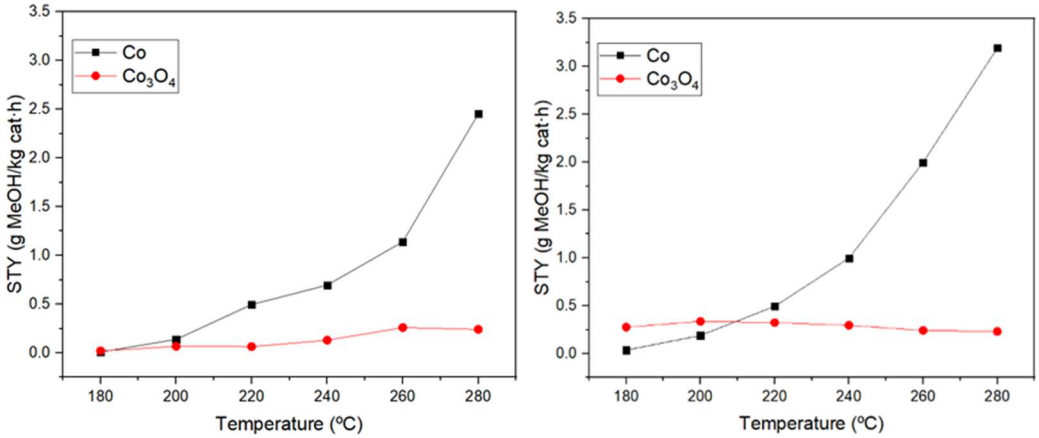

Figure 6. STY values for cobalt and cobalt oxide nanoparticles at a pressure of 10 bar (left) and 15 bar (right).

Two ways to improve the catalytic activity working with cobalt oxide nanoparticles were studied: (a) the addition of polyvinylpyrrolidone (PVP) to control the size of the nanoparticles, and (b) the addition of a support to improve the synergistic effect between the nanoparticles and the support. A comparison of the catalysts performance with and without PVP was carried out to analyse the effect of this polymer on the materials. By adding PVP in the synthesis of Co_3O_4, higher methanol STY was obtained which is accounted for by the smaller nanoparticles of Co_3O_4 with a more spherical morphology (Figure 4C and Figure 4D), leading to higher specific surface area and therefore more availability of the catalytic sites.

To study the effect of supports on the catalytic activity of Co_3O_4 nanoparticels, thye were immobilised on different supports inculding zeolite, CeO_2 and MnO_2. As seen in Figure 7, more methanol STY was obtained when immobilising Co_3O_4 on CeO_2. This can be attributed to the metal-support interaction between Co_3O_4 and CeO_2 generating interfacial sites which can synergystically catalyze methnaol synthesis reaction. In addition, oxygen vacancies present in CeO_2 are also assumedt to facilitate the adsorption and activation of carbon dioxide [20,21,34–36]. Other support studied was zeolite, which resulted in an improvement in methanol production since the presence of aluminum atoms in these silicate-based materials introduces negative charges that are compensated by exchangeable cations in the pore space, and these porous characteristics in the zeolite structure are those that allow greater carbon dioxide adsorption capacity [19,37]. Co_3O_4 immobilised on MnO_2 also resulted in more methanol STY compared to Co_3O_4. This can be attributed to the synergistic effects of the two materials as the catalytic activities of the individual materials are lower and less selective for methanol (Figure 6), indicating the importance of the architecture and nature of the interface [11]. Comparing the methanol STY of the three supports studied, CeO_2 performed the best as the support which can be due to the oxygen vacancies promoting carbon dioxide adsorption and activation as well as the generation of the interfacial sites betweeen CeO_2 and Co_3O_4 being more favorable for the methnaol syntheis reaction.

Preprints (www.preprints.org) | NOT PEER-REVIEWED | Posted: 31 October 2023 doi:10.20944/preprints202310.2044.v1

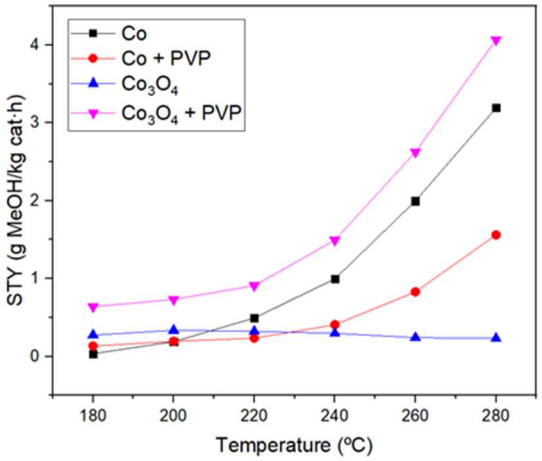

Figure 7. STY values for cobalt and cobalt oxide nanoparticles with and without PVP at 15 bar.

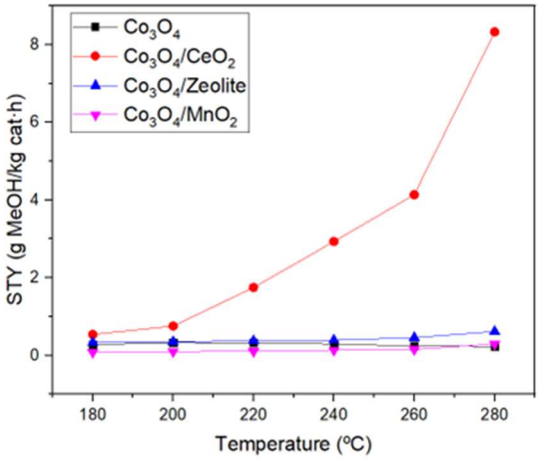

Figure 8. STY values for each catalyst at different temperatures and a pressure of 15 bar.

Methanol selectivity for the catalyst samples is presented in Figure 9. As can bee seen, at 180 ºC and 15 bar, the methanol selectivity for all samples was 100%, indicating that no carbon monoxide was formed at this temperature. However, as the temperature increases, the selectivity decreases as the enthalpy of methanol synthesis is negative, and therefore it is an exothermic reaction, which is more favoured at lower temperatures (Figure 9) [9,38]. In case of Co_3O_4 with PVP and Co_3O_4/zeolite, a decrease in selectivity towards methanol was only observed from 220 ºC. As for the other remaining catalysts, this methanol selectivity decreased considerably because of the production of carbon monoxide at high temperatrures (Figure 9) [11,39].

Preprints (www.preprints.org) | NOT PEER-REVIEWED | Posted: 31 October 2023 doi:10.20944/preprints202310.2044.v1

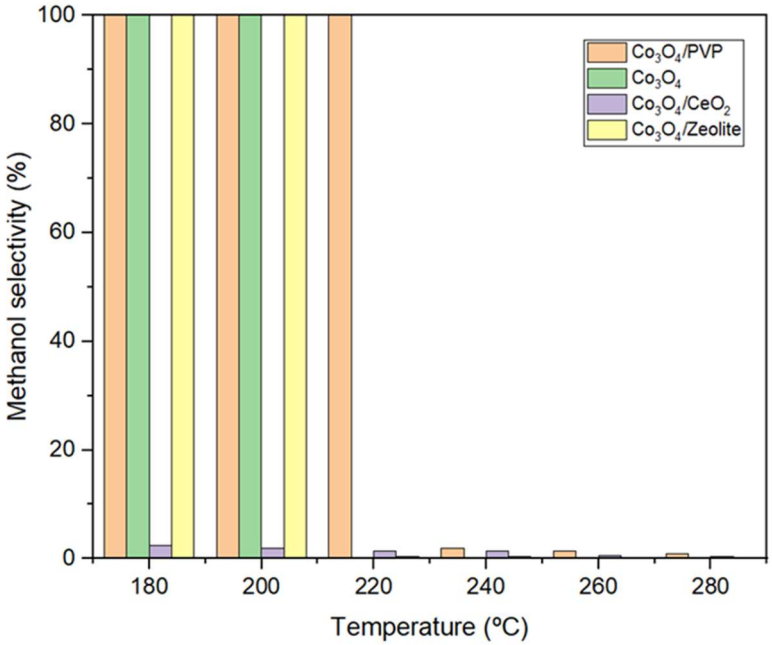

Figure 9. Methanol selectivity (%) values at 15 bar of the best catalysts.

4. Conclusions

In this work, a series of cobalt-based catalysts with different supports were synthesised and their catalytic activity for methanol syntheis from carbon dioxide hydrogenation was studied. XRD analysis detected the crystalline phase of the samples and confirmed the integration of Co_3O_4 and Co on the supports studied (zeolite, cerium oxide and manganese oxide). Moreover, it was demonstrated that the addition of PVP as a stabilising agent improves the catalytic capacity of Co_3O_4, as it helps to obtain more homogeneous and smaller nanoparticles. However, for the Co catalyst synthesized using PVP, this effect was not observed as a result of partial oxidation of the material due to the presence of the stabilizing agent. Comparing the effect of the supports studied, the performance of CeO_2 as support was more promisong which was accounted for by the presencec of oxygen vacancies in CeO_2 which promot carbon dioxide adsorption and activation. In addition, the higher catalytic activity of the catalyst supported by CeO_2 can be attributed to the genearation of favorbale interfacial sites betweeen CeO_2 and Co_3O_4 for the methnaol syntheis reaction.

Author Contributions: Conceptualization, A.S. and J.M.-V; methodology, A.C.G., Z.B.-A, S.A.V. and A.A.M.; validation, J.M.-V. and A.C.G.; formal analysis, A.C.G., J.M.-V. S.A.V., and A.A.M.; investigation, A.C.G. and J.M.-V.; resources, A.S. and J.M.-V.; data curation, A.C.G., Z.B.-A and A.A.M.; writing—original draft preparation, A.C.G.; writing—review and editing, A.C.G., J.M.-V., S.A.V., A.A.M. and A.S.; visualization, A.C.G.; supervision, J.M.-V. and A.S.; project administration, A.S.; funding acquisition, A.S. All authors have read and agreed to the published version of the manuscript.

Funding: This research was funded by Fundación Ramón Areces in the hallmark of the META2NOL project granted in the XIX National Contest of Life and Matter Sciences Projects, grant number CIVP19A5952. Anna Carrasco García thanks UAB for the PIF scholarship granted for the completion of her PhD thesis. Ahmad Abo Markeb thanks the Spanish Ministry of Universities for his Maria Zambrano scholarship.

Data Availability Statement: Not applicable.

Acknowledgments: Not applicable.

Conflicts of Interest: The authors declare no conflict of interest.

 doi:10.20944/preprints202310.2044.v1

References

1. Masson-Delmotte, V.; Zhai P.; Pirani A.; Connors S.L.; Péan C.; Berger S., Caud N., Chen Y. IPCC, **2021**: Summary of Policymakers. Contribution of Working Group I to the Sixth Assessment Report of the Intergovernmental Panel on Climate Change. En *Climate Change 2021: The Physical Science Basis*. Cambridge University Press, United Kingdom and New York, NY, USA **2021**, No. In Press, 3949.
2. Yadav, S.; Mondal, S.S. A review on the progress and prospects of oxy-fuel carbon capture and sequestration (CCS) Technology. *Fuel* **2022**, *308*, 122057.
3. Sabri, M.A.; Al Jitan, S.; Bahamon, D.; Vega, L.F.; Palmisano, G. Current and future perspectives on catalytic-based integrated carbon capture and utilization. *Sci. Total Environ.* **2021**, *790*, 148081.
4. Song, C. Global challenges and strategies for control, conversion and utilization of CO_2 for sustainable development involving energy, catalysis, adsorption and chemical processing. *Catal. Today* **2006**, *115*, 2-32.
5. Olah, G.A. Beyond Oil and Gas: The Methanol Economy. *Angew. Chemie Int. Ed.* **2005**, 44, 2636–2639.
6. Jadhav, S.G., Vaidya, P.D., Bhanage, B.M., Joshi, J.B. Catalytic carbon dioxide hydrogenation to methanol: A review of recent studies. *Chem. Eng. Res. Des.* **2014**, *92*, 2557–2567.
7. Li, M.M.J.; Tsang, S.C.E. Bimetallic catalysts for green methanol production via CO_2 and renewable hydrogen: A mini-review and prospects. *Catal. Sci. Technol.* **2018**, *8*, 3450–3464.
8. Sha, F.; Han, Z.; Tang, S.; Wang, J.; Li, C. Hydrogenation of Carbon Dioxide to Methanol over Non−Cu-based Heterogeneous Catalysts. *ChemSusChem* **2020**, *13*, 6160–6181.
9. Have, I.C.; Kromwijk, J.J.G.; Monai, M; Ferri, D., Sterk, E.B.; Meirer, F.; Weckhuysen, B.M. Uncovering the reaction mechanism behind CoO as active phase for CO_2 hydrogenation. *Nat. Commun.* **2022**, *13*, 324.
10. Tan, Q.; Shi, Z.; Wu, D. CO_2 Hydrogenation to Methanol over a Highly Active CuNi/CeO_2-Nanotube Catalyst. *Ind. Eng. Chem. Res.* **2018**, *57*, 10148–10158.
11. Stangeland, K.; Kalai, D.Y.; Ding, Y.; Yu, Z. Mesoporous manganese-cobalt oxide spinel catalysts for CO_2 hydrogenation to methanol. *J. CO_2 Util.* **2019**, *32*, 146–154.
12. Wang, L.; Guan, E.; Wang, Y.; Wang, L.; Gong, Z.; Cui, Y.; Meng, X.; Gates, B.C.; Xiao, F.S. Silica accelerates the selective hydrogenation of CO2 to methanol on cobalt catalysts. *Nat. Commun.* **2020**, 11, 1–9.
13. Zhou, Y.; Jiang, Y.; Qin, Z.; Xie, Q.; Ji, H. Influence of Zr, Ce, and La on Co_3O_4 catalyst for CO_2 methanation at low temperature. *Chinese J. Chem. Eng.* **2018**, 26, 768–774.
14. Suslova, E.V.; Chernyak, S.A.; Egorov, A.V.; Savilov, S.V.; Lunin, V.V. CO_2 hydrogenation over cobalt-containing catalysts. *Kinet. Catal.* **2015**, 56, 646–654.
15. Wang, L.; Wang, L.; Zhang, J.; Liu, X.; Wang, H.; Zhng, W.; Yang, Q.; Ma, J.; Dong, X.; Jo Yoo, S.; Kim, J.G.; Meng, X.; Xiao, F.S. Selective Hydrogenation of CO_2 to Ethanol over Cobalt Catalysts. *Angew. Chemie Int. Ed.* **2018**, *57*, 6104–6108.
16. Ouyang, B.; Xiong, S.; Zhang, Y.; Liu, B.; Li, J. The study of morphology effect of Pt/Co_3O_4 catalysts for higher alcohol synthesis from CO_2 hydrogenation. *Appl. Catal. A Gen.* **2017**, *543*, 189–195.
17. Tursunov, O.; Tilyabaev, Z. Hydrogenation of CO_2 over Co supported on carbon nanotube, carbon nanotube-Nb_2O_5, carbon nanofiber, low-layered graphite fragments and Nb_2O_5. *J. Energy Inst.* **2019**, *92*, 18–26.
18. Fan, T.; Liu, H.; Shao, S.; Gong, Y.; Li, G.; Tang, Z. Cobalt Catalysts Enable Selective Hydrogenation of CO_2 toward Diverse Products: Recent Progress and Perspective. *J. Phys. Chem. Lett.* **2021**, *12*, 10486–10496.
19. Carrasco Garcia, A.; Moral-Vico, J.; Markeb, A.A.; Sanchez, A. Conversion of Carbon Dioxide into Methanol Using Cu–Zn Nanostructured Materials as Catalysts. *Nanomaterials* **2022**, 12, 999.
20. Dou, J.; Tang, Y.; Nie, L.; Andolina, C.M.; Zhang, X.; House, S.; Li, Y.; Yang, J.; Tao, F. Complete Oxidation of Methane on Co_3O_4/CeO_2 Nanocomposite: A Synergic Effect. *Catal. Today* **2018**, *311*, 48–55.
21. Liu, X.; Zhou, K.; Wang, L.; Wang, B.; Li, Y. Oxygen vacancy clusters promoting reducibility and activity of ceria nanorods. *J. Am. Chem. Soc.* **2009**, 131, 3140–3141.
22. Javed, R.; Zia, M.; Naz, S.; Aisida, S.O.; ul Ain, N.; Ao, Q. Role of capping agents in the application of nanoparticles in biomedicine and environmental remediation: recent trends and future prospects. *J. Nanobiotechnology* **2020**, *18*, 1–15.
23. Zhao, Y.W.; Zheng, R.K.; Zhang, X.X.; Xiao, J.Q. A simple method to prepare uniform Co nanoparticles. *IEEE Trans. Magn.* **2003**, *39*, 2764–2766.
24. Worku, A.K.; Ayele, D.W.; Habtu, N.G.; Yemata, T.A. Engineering Co_3O_4/MnO_2 nanocomposite materials for oxygen reduction electrocatalysis. *Heliyon* **2021**, *7*, e08076.
25. Natile, M.M.; Glisenti, A. CoO x / CeO_2 Nanocomposite Powders : Synthesis, Characterization, and Reactivity," *Chem. Mater.* **2005**, *17*, 3403-3414.
26. Jincy, C.S.; Meena, P. Synthesis of Co_3O_4 nanoparticles for sensing toxic gas at room temperature. *Mater. Today Proc.* **2020**, 33, 2362–2365.
27. Wang, C.; Zhang, C.; Hua, W.C.; Guo, Y.; Lu, G.Z.; Gil, S.; Giroir-Fendler, A. Catalytic oxidation of vinyl chloride emissions over Co-Ce composite oxide catalysts. *Chem. Eng. J.* **2017**, *315*, 392–402.
28. Palacio, R.; Torres, S.; Lopez, D.; Hernandez, D. Selective glycerol conversion to lactic acid on Co_3O_4/CeO_2 catalysts. *Catal. Today* **2018**, 302, 196–202.

29. Feng, M.; Zhang, G.; Du, Q.; Su, L.; Ma, Z.; Qin, X.; Shao, G. Co_3O_4@MnO_2 core shell arrays on nickel foam with excellent electrochemical performance for aqueous asymmetric supercapacitor. *Ionics (Kiel)* **2017**, *23*, 1637–1643.
30. Davar, F.; Fereshteh, Z.; Shoja Razavi, H.; Razavi, R.S.; Loghman-Estarki, M.R. Synthesis and characterization of cobalt oxide nanocomposite based on the Co_3O_4–zeolite Y. *Superlattices Microstruct.* **2014**, *66*, 85–95.
31. Gupta, S.; Ciotonea, C.; Royer, S.; Dacquin, J.; Vinod, C.P. Engineering pore morphology using silica template route over mesoporous cobalt oxide and its implications in atmospheric pressure carbon dioxide hydrogenation to olefins. *Appl. Mater. Today* **2020**, *19*, 100586.
32. Jampaiah, D.; Damma, D.; Chalkidis, A.; Venkataswamy, P.; Bhargava, S.K.; Reddy, B.M. MOF-derived ceria-zirconia supported Co_3O_4 catalysts with enhanced activity in CO_2 methanation. *Catal. Today* **2020**, 356, 519-526.
33. Díez-Ramírez, J.; Sanchez, P.; Kyriakou; V.; Zafeiratos; S.; Marnellos, G.E.; Konsolakis, M.; Dorado, F. Effect of support nature on the cobalt-catalyzed CO_2 hydrogenation. *J. CO_2 Util.* **2017**, *21*, 562–571.
34. Gabe, A.; García-Aguilar, J.; Berenguer-Murcia, A.; Morallón, E.; Cazorla-Amorós, D. Key factors improving oxygen reduction reaction activity in cobalt nanoparticles modified carbon nanotubes. *Appl. Catal. B: Environ.* **2017**, *217*, 303-312.
35. Jiang, F.; Wang, S.; Liu, B; Liu, J; Wang, L.; Xiao, Y.; Xu, Y.; Liu, X. Insights into the Influence of CeO_2 Crystal Facet on CO_2 Hydrogenation to Methanol over Pd/CeO_2 Catalysts. *ACS Catal.* **2020**, *10*, 11493–11509.
36. Sha, F.; Han, Z.; Tang, S.; Wang, J.; Li, C. Hydrogenation of Carbon Dioxide to Methanol over Non−Cu-based Heterogeneous Catalysts. *ChemSusChem* **2020**, 13, 6160– 6181.
37. Choi, S.; Drese, J.H.; Jones, C.W. Adsorbent materials for carbon dioxide capture from large anthropogenic point sources. *ChemSusChem* **2009**, *2*, 796–854.
38. Ronda-Lloret, M.; Wang, Y.; Oulego, P.; Rothenberg, G.; Tu, X.; Shiju, N.R. CO_2 Hydrogenation at Atmospheric Pressure and Low Temperature Using Plasma Enhanced Catalysis over Supported Cobalt Oxide Catalysts. *ACS Sustain. Chem. Eng.* **2020**, *8*, 17397–17407.
39. Li C.S.; Melaet, G.; Ralston, W.T.; An, K.; Brooks; C.; Ye, Y.; Liu, Y.S.; Zhu, J.; Guo, J.; Alayoglu, S.; Somorjai, G.A.. High-performance hybrid oxide catalyst of manganese and cobalt for low-pressure methanol synthesis. *Nat. Commun.* **2015**, *6*, 1–5.